Agricultural and Forest Meteorology 150 (2010) 1147–1153

Contents lists available at ScienceDirect

Agricultural and Forest Meteorology

journal homepage: www.elsevier.com/locate/agrformet

Latent heat in soil heat flux measurements

J.L. Heitman[a,*], R. Horton[b], T.J. Sauer[c], T.S. Ren[d], X. Xiao[b]

[a] Soil Science Department, North Carolina State University, Campus Box 7619, Raleigh, NC 27695, USA
[b] Agronomy Department, Iowa State University, Ames, IA 50011, USA
[c] USDA-ARS Nat'l Lab. Agriculture and Environment, Ames, IA 50011, USA
[d] Soil and Water Department, China Agricultural University, Beijing 100193, PR China

ARTICLE INFO

Article history:
Received 16 February 2010
Received in revised form 19 April 2010
Accepted 24 April 2010

Keywords:
Soil heat flux
Latent heat flux
Surface energy balance

ABSTRACT

The surface energy balance includes a term for soil heat flux. Soil heat flux is difficult to measure because it includes conduction and convection heat transfer processes. Accurate representation of soil heat flux is an important consideration in many modeling and measurement applications. Yet, there remains uncertainty about what comprises soil heat flux and how surface and subsurface heat fluxes are linked in energy balance closure. The objective of this study is to demonstrate the presence of a subsurface latent heat sink, which must be considered in order to accurately link subsurface heat fluxes between depths near and at the soil surface. Measurements were performed under effectively bare surface conditions in a silty clay loam soil near Ames, IA. Soil heat flux was measured with heat-pulse sensors using the gradient heat flux approach at 1-, 3-, and 6-cm soil depths. Independent estimates of the daily latent heat sink were obtained by measuring the change of mass of microlysimeters. Heat flux measurements at the 1-cm depth deviated from heat flux measurements at other depths, even after calorimetric adjustment was made. This deviation was most pronounced shortly after rainfall, where the 1-cm soil heat flux measurement exceeded 400 W m^{-2}. Cumulative soil heat flux measurements at the 1-cm depth exceeded measurements at the 3-cm depth by >75% over a 7-day rain-free period, whereas calorimetric adjustment allowed 3- and 6-cm depth measurements to converge. Latent heat sink estimates from the microlysimeters accounted for nearly all of the differences between the 1- and 3-cm depth heat flux measurements, indicating that the latent heat sink was distributed between the 1- and 3-cm depths shortly after the rainfall event. Results demonstrate the importance of including latent heat when attempts are made to link or extrapolate subsurface soil heat flux measurements to the surface soil heat flux.

1. Introduction

Accurate determination of surface soil heat flux is an important consideration in applications ranging from mesoscale land surface modeling (McCumber and Pielke, 1981), to field-scale energy balance in Bowen ratio (Passerat de Silans et al., 1997) and eddy covariance techniques (Shao et al., 2008), to characterizing local temperature variations within managed and natural systems (e.g., Kustas et al., 2000; Kluitenberg and Horton, 1990). Techniques for determining soil heat flux also vary, including both direct measurement (e.g., Ochsner et al., 2006) and estimation based on soil profile temperature distributions (e.g., Horton and Wierenga, 1983) or other measured parameters (e.g., Daughtry et al., 1990). Sauer and Horton (2005) reviewed a variety of techniques that have come to be considered de facto standards for determining soil heat flux, including heat flux plates and the combination method. Yet, there remains uncertainty about what comprises soil heat flux and how surface and subsurface heat flux are linked in energy balance closure (Passerat de Silans et al., 1997; Heusinkveld et al., 2004; Holmes et al., 2008; Wang and Bras, 2009; Holmes et al., 2009).

Some confusion about soil heat flux likely arises from the coupling of water and energy transfer in near surface soil. In describing fully coupled soil heat and water transfer theory, Milly (1982) and Passerat de Silans et al. (1989) used apparent thermal conductivity as a combined term linking simple conduction with latent heat transport by vapor diffusion (i.e., latent heat flux) to describe soil heat flux. However, this fully coupled approach is often absent from implementation and interpretation for pragmatic field measurement campaigns aimed at describing surface energy balance, i.e., soil heat flux is often treated as simple conduction.

When soil heat flux is measured at a subsurface depth, correction for heat terms between the surface and the measurement depth is necessitated, i.e., the commonly used combination method (Fuchs and Tanner, 1968) includes correction for sensible heat storage in the soil layer between the measurement depth and the soil surface, based on temperature change with time and soil heat

* Corresponding author. Tel.: +1 919 513 1593; fax: +1 919 515 2167.
E-mail address: jlheitman@ncsu.edu (J.L. Heitman).

0168-1923/$ – see front matter © 2010 Elsevier B.V. All rights reserved.
doi:10.1016/j.agrformet.2010.04.017

capacity. Massman (1993) indicated that heat flux estimates could include errors up to 10% of the total heat flux when inaccurate estimates of the soil condition are used to determine this heat storage term. Ochsner et al. (2007) suggested that, when neglecting the heat storage term, soil heat flux measured at the 6-cm soil depth might underestimate surface heat flux by more than 50%. Owing to concerns with the link between surface and subsurface heat flux, Heusinkveld et al. (2004) suggested "burying the sensor as close to the surface as possible" in dry, bare soil with a very high surface heat flux. However, the presence of a drying front may limit such an installation approach in conditions where subsurface soil moisture, and hence latent heat of vaporization of soil water, is important (Sauer and Horton, 2005). Improved measurements of soil temperature and soil heat capacity can account directly for sensible heat storage, but not directly for latent heat.

de Vries and Philip (1986) discussed considerations for determining soil heat flux at multiple depths in the null-alignment method. They acknowledged the possibility of a subsurface latent heat sink and argued for its important impact on accurately calculating soil heat flux with depth. Their argument was based on local average soil water evaporation rates and divergence in the subsurface temperature gradient. Mayocchi and Bristow (1995) reiterated this argument, and using an estimated strength of the latent heat flux term from de Vries and Philip (1986), demonstrated subsurface energy balance closure. Though these arguments may indeed be valid, they are based primarily on approximation of unmeasured subsurface terms (i.e., latent heat and soil heat flux).

Debate about the presence of subsurface heat sink terms remains active as estimates of soil heat flux are required in new applications such as remote sensing. Holmes et al. (2008) use an approximated subsurface heat sink term, which they attribute to both sensible and latent heat components of the surface energy balance, to link surface temperatures to subsurface temperature distributions. Using a fitting approach, they concluded that these subsurface terms must be included to describe how the surface heat flux propagates through the profile. Their approach was questioned by Wang and Bras (2009), who argued that this description of the soil heat flux was invalid, particularly the use of a subsurface sensible heat flux that coincided with a surface sensible heat flux term. Further explanation of terms was provided in Holmes et al. (2009).

Overall, the understanding of how subsurface soil heat fluxes are linked to the soil surface would be improved by some clear, measurements and analysis indicating the presence of a subsurface heat sink. The objective of this report is to illustrate the presence of a subsurface latent heat sink, which must be considered in order to accurately link subsurface heat fluxes between depths near the soil surface. Measurements of subsurface soil heat flux and independent measurements of soil water evaporation (i.e., the latent heat sink) are used to demonstrate this connection.

2. Materials and methods

2.1. Field site

Measurements were obtained at a field site located near Ames, IA (41°N, 93°W). Soil at the site is mapped as Canisteo silty clay loam (Fine-loamy, mixed, superactive, calcareous, mesic Typic Endoaquolls) with slopes ≤3%. Fall chisel plow tillage in combination with secondary tillage in the spring was used to prepare the field for planting prior to the experiments. Soil bulk density in the surface horizon was measured as 1.29 Mg m^{-3} post-tillage. Soybean was planted with 0.76 m row spacing on day of year (DOY) 131 in north-south oriented rows; emergence occurred on DOY 138-139. The measurement period discussed below occurred between DOY 142 and 161. Plant heights were determined on 2 days proximate to this period; heights were approximately 5.6 and 8.7 cm on DOY 152 and 159, respectively, based on an average of 209 plants each day. At this size, soybean root growth in the plant inter-row is considered minimal (cf. Mitchell and Russell, 1971). Because plants were small, the field site can be considered to be effectively bare. An adjacent long-term field study approximately 60 m from the instrumentation nest, within the same field, provided ancillary data including precipitation (tipping bucket gage), net radiation (four-component net radiometer; CNR 1, Kipp and Zonen, Delft, the Netherlands at 1.2 m above the soil surface), and soil water content at the 0–6-cm depth increment (Theta Probe Model ML2x, Dynamax, Inc., Houston, TX, USA).

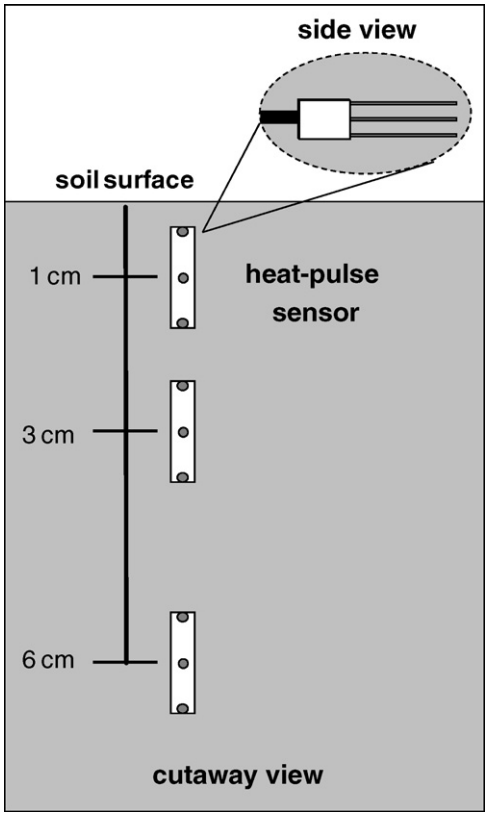

Fig. 1. Heat-pulse sensor installation. The cutaway view is drawn approximately to scale. The installation was repeated at three positions.

2.2. Heat flux measurements

Heat-pulse (HP) sensors built following the design of Ren et al. (2003) were used for soil heat flux measurement. The sensors consisted of three stainless steel needles (1.3 mm diam., 4 cm length) fixed approximately 6 mm apart with an epoxy body at one end. Each needle contained a Type E thermocouple for measuring temperature; the central needle also contained a resistance heater for generating a heat-pulse. The sensors were calibrated in agar stabilized water to determine the apparent distance between the needles (Campbell et al., 1991). The sensors were installed on DOY 140 via a 10 cm deep access trench by pushing the needles from the trench into undisturbed soil. HP sensors were installed at three depths in each profile, centered at 1, 3, and 6 cm, with the plane of the needles oriented perpendicular to the soil surface (Fig. 1). This installation was repeated at three adjacent locations (quarter row, mid row, and three-quarter row) for a total of nine sensors. After installation, the sensor lead wires were routed through the trench and the trench was carefully backfilled with soil. The sensors were connected to a data acquisition system on the soil surface,

which consisted of a datalogger (CR23X, Campbell Sci., Logan, UT) and multiplexers for the thermocouples and heaters, all housed in a weatherproof enclosure. Power was supplied by a 12 V battery maintained with a solar panel. All heaters were controlled and measured with a single control circuit consisting of a relay and 1-Ω precision resistor.

Thermal property measurements were collected each 3 h. Thermal diffusivity k ($m^2\,s^{-1}$) and soil volumetric heat capacity C ($J\,m^{-3}\,°C^{-1}$) were determined following the procedures described by Bristow et al. (1994) and Knight and Kluitenberg (2004), respectively. Measurements were corrected for ambient temperature drift using the temperature measurements collected prior to HP initiation (Jury and Bellantouni, 1976; Ochsner et al., 2006). Soil thermal conductivity λ ($W\,m^{-1}\,°C^{-1}$) was computed as $\lambda = kC$. Thermocouples in each sensor needle were also used to record ambient soil temperature each 30 min (5-min average) at depths of 4, 10, 16, 24, 30, 36, 54, 60, and 66 mm; a separate thermocouple was placed at the 10 cm depth in each profile to record ambient temperature. These data were combined with λ measurements to calculate gradient-based soil heat flux G ($W\,m^{-2}$) at 1, 3, and 6 cm, where the temperature gradients were determined as the temperature difference ΔT (°C) between outer needles of a given probe (e.g., 4 and 16 mm depths for the 1-cm probe) divided by the calibrated distance Δz (m) between the needles ~12 mm (Ochsner et al., 2006):

$$G = -\lambda \frac{\Delta T}{\Delta z} \quad (1)$$

Because soil temperatures were measured more frequently (each 30 min) than λ (each 3 h), a time-weighted average was used to determine λ for 30-min time steps between observations. This allowed estimation of G each 30 min.

As discussed in the following, soil temperature data and measured C were also used to make calorimetric corrections for changes in sensible heat storage following the approach of Fuchs (1986) and Ochsner et al. (2007):

$$\Delta S = \sum_{i=1}^{N} C_{i,j-1} \frac{T_{i,j} - T_{i,j-1}}{t_j - t_{j-1}} (z_i - z_{i-1}) \quad (2)$$

where ΔS ($W\,m^{-2}$) is the change in sensible heat storage, T (°C) is temperature, t (s) is time, z (m) is depth, and the subscripts i and j are index variables for depth (layers) and time steps, respectively. Time-weighted averages of C were used to allow estimates of ΔS for 30-min intervals.

2.3. Microlysimeter measurements

Weighable microlysimeters (MLs) were used to collect estimates of water loss from the soil through evaporation. The MLs were built following recommendations by Evett et al. (1995). The MLs consisted of white polyvinyl chloride pipe with 7.6-cm ID (3-mm wall thickness), cut to a 10-cm length. Eight replicate MLs were installed along each of five transects within the study area; transects were positioned midway between adjacent plant rows. The MLs were installed using a drop hammer so that the top of the ML was flush with the soil surface. Installation was completed approximately 12 days before measurements, which allowed several wetting and drying cycles in the soil before their use. On selected days, one ML was carefully excavated from each of the transects. The MLs were then shaved to remove excess soil, and bottoms were capped with plastic bags. The capped MLs were then weighed in the field with a portable balance (±0.01 g) and returned to their original position, with surrounding soil carefully repacked so that the MLs were flush with the soil surface. After 24 h, the capped MLs were again removed from the surrounding soil and reweighed to determine their change in mass. Each ML was used for 1–2 days during which time no rainfall occurred. All mass change was attributed to loss of water via net evaporation.

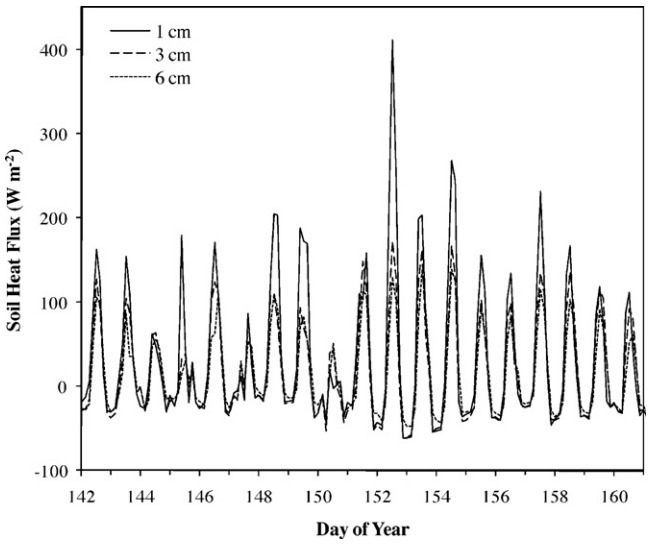

Fig. 2. Soil heat flux observations at 1 cm, 3 cm, and 6 cm soil depths.

The quantity of latent heat associated with soil water evaporation per unit area ($J\,m^{-2}$) was estimated using mass loss from the MLs during each 24-h measurement period. Mass loss per cross-sectional area of the ML ($Mg\,m^{-2}$) was divided by the density of water (~1 $Mg\,m^{-3}$) to give a volume per cross-sectional area ($m^3\,m^{-2}$). This volume per unit area was, in turn, multiplied by the latent heat (L_o, $J\,m^{-3}$) required for phase change (Horton, 1989):

$$L_o = 2.495 \times 10^9 - 2.247 \times 10^6\, T_m \quad (3)$$

where T_m (°C) is the mean temperature for the soil depth increment (determined as a daily mean from thermocouple data).

3. Results and discussion

3.1. Soil heat flux observations

Mean subsurface soil heat flux measurements (1, 3, and 6 cm depth) from sensor activation (DOY 142) through DOY 161 are shown in Fig. 2. As described above, this corresponds to the period shortly after soybean emergence, with plant heights <9 cm (i.e., effectively bare soil in the inter-rows). Deviation amongst the sensors at each row position for a given depth was generally small (data not shown); median standard deviations for a given time and depth were 6.9, 2.9, and 1.9 $W\,m^{-2}$ at the 1, 3, and 6 cm depths, respectively. This variation was attributed primarily to slight differences in vertical position of the sensors associated with installation near the uneven soil surface after tillage and planting. Ham and Kluitenberg (1993) showed positional variation in soil heat flux across the row with soybean heights of 0.58 m and taller. No positional pattern was observed between the three inter-row positions with the smaller plants in the present data set. Thus, mean values from the three positions were used for all subsequent analysis.

Soil heat flux shows typical diurnal variation at all measured depths (Fig. 2). Rainfall occurred on 4 days during the period; dampening in the daily wave is apparent on DOY 144, 147, and 150, associated with these rainfall events (Fig. 3). Despite a rainfall event, DOY 145 differs slightly from this pattern because rainfall occurred at midday after heat flux had begun to increase. On the remaining days without rainfall, there is clear ordering with the largest amplitude of the daily wave apparent at the 1-cm depth followed by the 3-cm depth. Differences in peak daily heat flux at

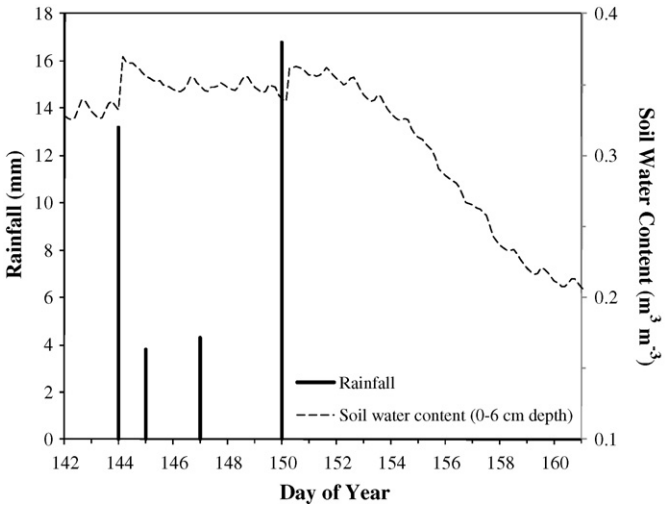

Fig. 3. Rainfall and soil water content (0–6 cm depth increment). Note that rainfall is represented as daily total on each day.

the 3- and 6-cm depths are <10% on all days, with maximum daily heat fluxes typically between 75 and 125 W m^{-2} at both depths. The difference between the 1- and 3-cm is more pronounced, with heat fluxes at the 1-cm depth as much as 50% larger than at the 3-cm depth on several days.

The maximum observed heat fluxes at the 1-cm depth exceeded 200 W m^{-2} on 5 days during the period shown in Fig. 2. However, these days do not necessarily correspond to days with highest net radiation (Fig. 4). Maximum daily net radiation was at or above 600 W m^{-2} on 10 of 19 days during the period, but two of the five largest soil heat fluxes were observed on days when net radiation was <550 W m^{-2} (DOY 148 and 152). Both days follow shortly after rainfall events. Of particular note is the large soil heat flux (>400 W m^{-2}) observed at the 1-cm depth on DOY 152, which constitutes just under 75% of the net radiation on that day. This large soil heat flux appears to be the product of high thermal conductivity following the preceding rainfall and increasing temperatures near the soil surface. The relatively large water content in the shallow soil, due to rainfall on DOY 150, begins to decline steadily after DOY 152 (Fig. 3). While not as apparent from the soil moisture data, which integrate soil moisture over the 0–6-cm depth increment, soil thermal conductivity at the 1-cm depth is in rapid decline from

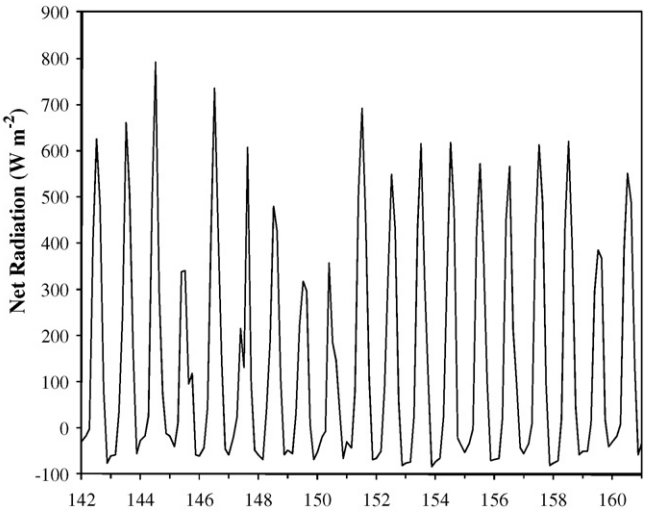

Fig. 4. Net radiation measured at 1.2 m above the soil surface.

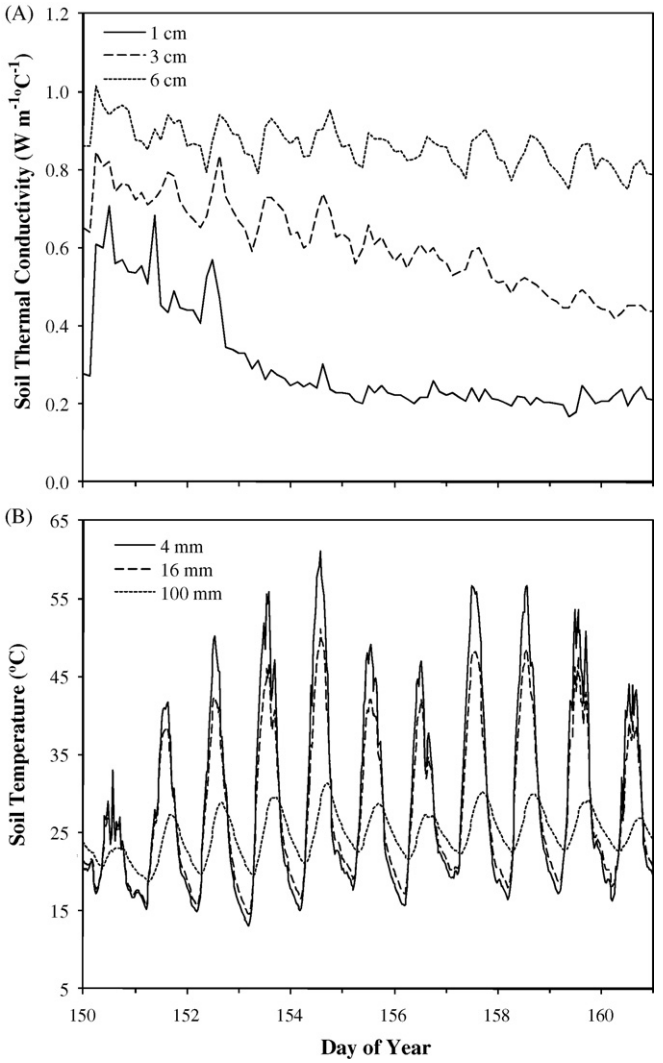

Fig. 5. Soil thermal conductivity at 1 cm, 3 cm and 6 cm soil depths (A) and soil temperature at 4 mm, 16 mm, and 100 mm (B).

soil drying by DOY 152 (Fig. 5A); thermal conductivities at the 3- and 6-cm depth increments are shown in the figure for comparison. Despite this decline, thermal conductivity at the 1-cm depth remains relatively high (approximately 50% higher) on DOY 152 compared to the subsequent period after DOY 153. At the same time, soil temperature is increasing and becoming more divergent with depth near the soil surface by DOY 152 (Fig. 5B). The maximum observed thermal gradient (i.e., temperature difference) between 4- and 16-mm depths is similar from DOY 152 to 159. However, the combination of large thermal gradient and high thermal conductivity were not observed on days subsequent to DOY 152. Thus, though this soil heat flux appears to be large compared to other days and other depths, it follows plausibly from temperature and thermal property observations.

3.2. Comparison of heat flux between measurement depths

While heat flux was measured at multiple depths in the present study, a typical approach in most studies is to measure the soil heat flux at a single depth and then use a calorimetric (i.e., combination) approach to determine heat flux at other depths or the soil surface. Volumetric heat capacity and ambient temperature data available from the HP sensors allow calculation of the change in soil sensible heat storage between the depths of heat flux measurement (Eq. (2)),

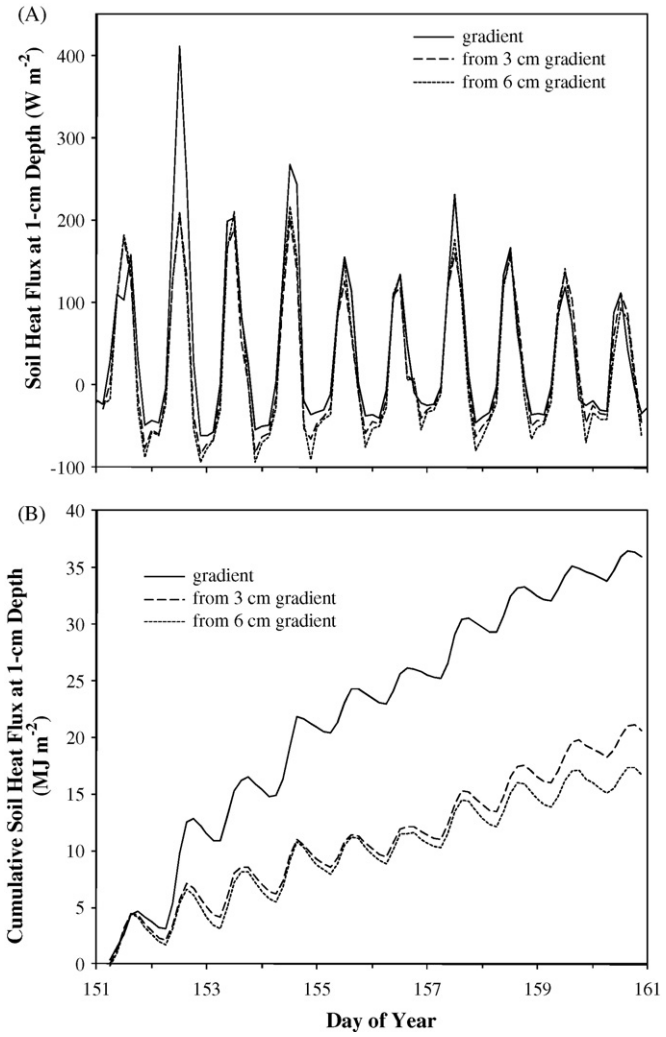

Fig. 6. Soil heat flux (A) and cumulative soil heat flux (B) at 1-cm soil depth determined from three approaches.

which in turn allows direct comparison of soil heat flux estimates based on correction to a common depth. Here, we use gradient heat flux determined from measurements at each depth (1, 3, and 6 cm) via Eq. (1) and the change in sensible heat storage between heat flux measurements depths is determined via Eq. (2). We make this comparison based on the shallowest measurement depth, 1 cm, for the rain-free period from DOY 150-161. Fig. 6A shows soil heat flux estimated at the 1-cm soil depth based on three approaches: (i) gradient measurement (i.e., identical to that shown in Fig. 2), (ii) 3-cm gradient measurement with soil sensible heat storage change between the 1- and 3-cm depths, and (iii) 6-cm gradient measurement with sensible heat storage change between the 1- and 6-cm depths.

By comparison to Fig. 2, Fig. 6A indicates improved agreement between maximum daily soil heat flux estimates once the sensible heat storage corrections are included. On most days maximum daytime heat flux is within 25 W m^{-2} for each estimate, though some exceptions occur on DOY 152, 154, and 157, which also had the largest observed heat fluxes. Nighttime heat fluxes appear to differ slightly more than in Fig. 2, with the storage term implying a larger magnitude to the nighttime heat flux determined from measurements at 3- and 6-cm, but differences remain $\leq$25 W m^{-2}. Another assessment of differences between estimates is to compare cumulative heat fluxes (Fig. 6B). As would be expected from previous comparisons, cumulative heat flux measured directly at the 1-cm soil depth begins to deviate markedly from other heat flux estimates on DOY 152. This deviation continues to grow thereafter with cumulative heat flux at the 1-cm depth exceeding heat flux estimates from measurements at 3- and 6-cm by more than 75% within 10 days (i.e., by DOY 161). Heat flux estimates based on 3- and 6-cm measurement depths differ only slightly from each other over this same period, with a difference of approximately 25%; most of this difference occurs after DOY 157. The calorimetric adjustment brings measurements from 3- and 6-cm depths into close agreement, but does not provide the same level of agreement between 1- and 3-cm measurements. This difference suggests an additional energy sink between the 1- and 3-cm depths.

Table 1
Daily evaporation and latent heat determined from microlysimeters.

DOY	Evaporation		
	Depth[a] (mm)	Coeff. var. (%)	Latent heat (MJ m^{-2})
151	3.9	7.0	9.6
152	1.6	14	4.0
153	1.4	19	3.3
154	1.3	22	3.2
155	1.1	27	2.6
156	0.65	39	1.6
157	1.3	11	3.1

[a] Volume per unit area; mean of five measurements.

3.3. Latent heat sink

Microlysimeter data were available on 7 consecutive days from DOY 151-157, which corresponded to the dry-down following rainfall on DOY 150. Means and coefficients of variations for the replicate MLs collected on each day are shown in Table 1. The total amount of net water evaporation for this 7-day period, approximately 1.1 cm, corresponds to the observed 0.12 cm cm^{-1} decline in soil water storage from soil water content sensor readings (Fig. 2). Variability amongst replicate microlysimeters averaged <20%, but increased as the soil dried. These data were used with Eq. (3) to estimate the latent heat sink associated with water vaporization, also shown in Table 1.

The latent heat flux constitutes one of four terms in the common surface energy balance:

$$\text{Net radiation} - \text{soil heat flux} = \text{sensible heat flux} + \text{latent heat flux}$$

The left side of this relationship (net radiation—soil heat flux) is often termed available energy. Disparity in soil heat flux between direct measurement at the 1-cm depth and estimates based on measurements at deeper depths (i.e., 3 or 6 cm), adjusted for soil heat storage change, provides two alternate approaches for calculating available energy with the net radiation data. Estimates of accumulated daily available energy based on the 1-cm depth and 3-cm depth measurements are shown in Fig. 7 together with daily latent heat totals from the MLs.

Estimates of available energy vary between 12.5 and 7.2 MJ m^{-2} based on the 1-cm depth soil heat flux measurements (Fig. 7). The variation is much smaller, between 12.5 and 11.2 MJ m^{-2}, for available energy estimates based on the 3-cm depth soil heat flux measurement. Most of the daily variation in available energy based on the shallower measurement comes from variation in soil heat flux, because net radiation is relatively consistent throughout the period (Fig. 4). When comparing the two estimates of available energy, it can also be noted that there is little difference in available energy estimates on DOY 151, immediately after rainfall on DOY 150. However, thereafter differences are more pronounced, exceeding 1.3 MJ m^{-2} on each day.

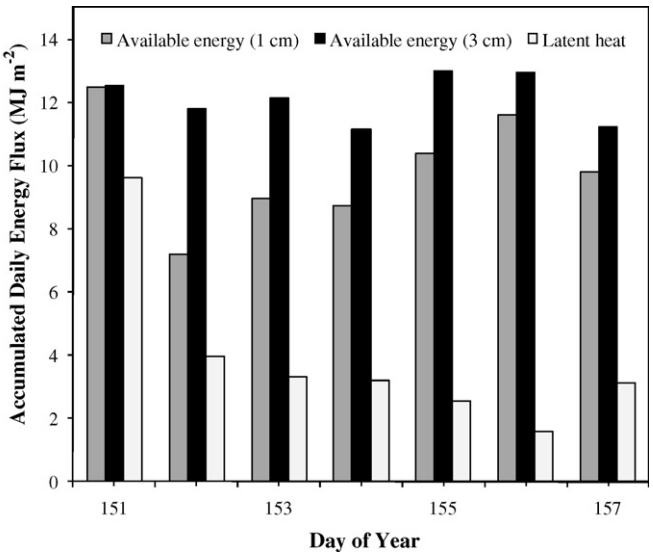

Fig. 7. Accumulated daily available energy and latent heat. Separate estimates of available energy were computed based on soil heat flux estimates from measurements at the 1- and 3-cm depths, as indicated in the legend.

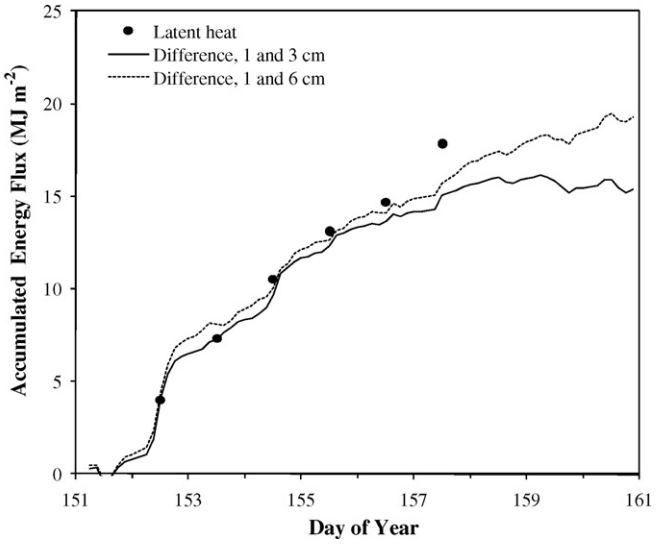

Fig. 8. Accumulated differences in soil heat flux and latent heat.

The latent heat total is largest on DOY 151, as would be expected owing to a high rate of evaporation following rainfall, and then decreases markedly on DOY 152 and more subtly thereafter (Fig. 7). This pattern in latent heat flux is consistent with falling rate evaporation associated with the transition from atmospherically- to soil-limited stages. With time, a larger fraction of available energy would be expected to partition to sensible heat flux as water availability for evaporation declines. Accompanying this shift, the evaporation zone presumably shifts from the soil surface to the subsurface. Thus, on DOY 151 while soil moisture supply remains high, the latent heat sink would be expected to occur very near the soil surface. Thereafter, the latent heat sink likely occurs deeper in the subsurface.

Examination of Fig. 7 reveals that the differences between the two available energy estimates and the magnitude of the latent heat sink are similar after DOY 151. This suggests that the difference between these two estimates of available energy may be that the shallow (i.e., 1-cm depth) estimate actually includes the latent heat sink term. If the latent heat sink is occurring below the 1-cm depth after DOY 151, the 1-cm depth soil heat flux measurement actually represents sensible soil heat flux + latent soil heat flux. Whereas, the 3-cm heat flux measurement (including heat storage adjustment) represents the sensible soil heat flux as portrayed in the common surface energy balance.

Further comparison amongst heat fluxes based on each depth is provided in Fig. 8. Here we take the cumulative difference between heat fluxes measured at the 1- and 3-cm depths, as well as the cumulative difference between the heat fluxes measured at the 1- and 6-cm depths, i.e., subtraction between fluxes shown in Fig. 6B. Noting that the latent heat sink likely occurs at a depth shallower than 1-cm on DOY 151, latent heat from DOY 151 is not included in the total.

Comparison between differences at measurement depths and the latent heat sink reveals that much of the difference between depths can be attributed to the presence of a latent heat sink. Because the difference between 3- and 6-cm measurements can be explained primarily through heat storage adjustment (Fig. 6), it is reasonable to assume that the latent heat sink occurs between the 1- and 3-cm depths on DOY 152-156. Thereafter, as the evaporation front proceeds downward, there is some disparity between measurements at the 3- and 6-cm depths. Latent heat sink estimates also begin to deviate a bit more from depth differences in soil heat flux on DOY 157 (Fig. 8). Though evaporation data for the period after DOY 156 are limited to only one observation, the preceding pattern might suggest that a more diffuse evaporation zone (i.e., latent heat sink) begins to extend below the 3 and even 6-cm depths by DOY 157.

Overall, these data indicate clearly a latent sink below the 1-cm soil depth, and that care must be taken when considering the choice of soil heat flux measurement depth for energy balance closure. If the energy balance is to be treated as presented in the common surface energy balance, soil heat flux must be measured at a depth below the soil-water evaporation zone. Soil heat flux measured at shallow depths may include heat that is partitioned to latent heat in the soil subsurface, and this partitioning would not be easily detected from heat flux measurements at a single depth. Such a situation would, in turn, limit attempts at energy balance closure by mis-representing individual energy balance terms. In the present data set, under the constraints of the common surface energy balance, it appears that soil heat flux measurement depth should exceed 3-cm below the soil surface; measurements as deep as 6-cm are necessary to provide some confidence that the evaporation zone is fully above the measurement depth for the 10-day rain-free period. In situations where the latent heat flux term is negligible and/or soil water storage and evaporation are minimal, shallower measurement depths may be possible (e.g., Heusinkveld et al., 2004). Extrapolation or interpolation of heat flux observations between depths should also be performed cautiously by explicitly accounting for the location and strength of the latent heat flux.

4. Summary and conclusions

Soil heat flux is considered a routine component for many energy balance applications, yet there remains considerable discussion and uncertainty in the literature about exactly what constitutes soil heat flux. Because soil heat flux is commonly measured below the surface, it is important to carefully consider how this subsurface heat flux is connected to the surface heat flux (as represented in the common surface energy balance), as well as to the heat fluxes at other non-measured depths. It has been proposed that a latent heat sink term must be included to properly link surface and subsurface heat flux. But the presence of this term/sink has not previously been shown directly from measurements. The goal of this report is to provide clear evidence

of a subsurface latent heat sink using simple measurement and analysis techniques. Gradient heat flux measurements at multiple depths indicate differences between subsurface heat flux measurements even after a calorimetric (sensible heat storage) adjustment is made. Using independent measurements of the latent heat sink for conditions during a field drying cycle, we demonstrate that differences in subsurface heat flux measurements can be readily explained by including latent heat. How this term is included will depend on the application (e.g., local energy balance studies) and measurement environment (moist vs. humid, soil type, etc.), but clearly the presence of a subsurface heat sink must be carefully considered when attempting to extrapolate subsurface soil heat flux measurements to estimate the surface soil heat flux or to make calculations of heat flux distribution with depth. For soil heat flux measurements in a moist environment with fine-textured soils, as in the present data set, we recommend that a reference soil heat flux measurement be collected 6 cm or deeper within the soil in order to calculate the surface heat flux term as it is commonly used in the energy balance equation.

Acknowledgement

The authors gratefully acknowledge the National Science Foundation for supporting this work through NSF Award No. 0809656. Work was also supported by the Chinese Academy of Sciences Visiting Professorship for Senior International Scientists, Award No. 2009Z2-37.

References

Bristow, K.L., Kluitenberg, G.J., Horton, R., 1994. Measurement of soil thermal properties with a dual-probe heat-pulse technique. Soil Sci. Soc. Am. J. 58, 1288–1294.
Campbell, G.S., Calissendorff, C., Williams, J.H., 1991. Probe for measuring soil specific heat using a heat-pulse method. Soil Sci. Soc. Am. J. 55, 291–293.
Daughtry, C.S.T., Kustas, W.P., Moran, M.S., Pinter, P.J., Jackson, R.D., Brown, P.W., Nichols, W.D., Gay, L.W., 1990. Spectral estimates of net radiation and soil heat flux. Remote Sens. Environ. 32, 111–124.
de Vries, D.A., Philip, J.R., 1986. Soil heat flux, thermal conductivity, and the null alignment method. Soil Sci. Soc. Am. J. 50, 12–18.
Evett, S.R., Warrick, A.W., Matthias, A.D., 1995. Wall material and capping effects on microlysimeter temperatures and evaporation. Soil Sci. Soc. Am. J. 59, 329–336.
Fuchs, M., 1986. Heat flux. In: Klute, A. (Ed.), Methods of Soil Analysis. Part I. Physical and Mineralogical Methods, 2nd ed. Am. Soc. Agron., Madison, WI, pp. 957–968.
Fuchs, M., Tanner, C.B., 1968. Calibration and field test of soil heat flux plates. Soil Sci. Soc. Am. Proc. 32, 326–328.
Ham, J.M., Kluitenberg, G.J., 1993. Positional variation in the soil energy balance beneath a row-crop canopy. Agric. Forest Meteorol. 63, 73–92.
Heusinkveld, B.G., Jacobs, A.F.G., Holtslag, A.A.M., Berkowicz, S.M., 2004. Surface energy balance closure in an arid region: role of soil heat flux. Agric. Forest Meteorol. 122, 21–37.
Holmes, T.R.H., Owe, M., De Jeu, R.A.M., Kooi, H., 2008. Estimating the soil temperature profile from a single depth observation: a simple empirical heatflow solution. Water Resour. Res. 44, W02412.
Holmes, T.R.H., Kooi, H., De Jeu, R.A.M., Owe, M., 2009. Reply to comment by J. Wang and R.L. Bras on "Estimating the soil temperature profile from a single depth observation: a simple empirical heatflow solution". Water Resour. Res. 45, WROO7513.
Horton, R., 1989. Canopy shading effects on soil heat and water flow. Soil Sci. Soc. Am. J. 53, 669–679.
Horton, R., Wierenga, P.J., 1983. Estimating the soil heat flux from observations of soil temperature near the surface. Soil Sci. Soc. Am. J. 47, 14–20.
Jury, W.A., Bellantouni, B., 1976. A background temperature correction for thermal conductivity probes. Soil Sci. Soc. Am. J. 40, 608–610.
Kluitenberg, G.J., Horton, R., 1990. Analytical solution for two-dimensional heat conduction beneath a partial surface mulch. Soil Sci. Soc. Am. J. 54, 1197–1206.
Knight, J.H., Kluitenberg, G.J., 2004. Simplified computational approach for the dual-probe heat-pulse method. Soil Sci. Soc. Am. J. 68, 447–449.
Kustas, W.P., Prueger, J.H., Hattfield, J.L., Ramalingam, K., Hipps, L.E., 2000. Variability in soil heat flux from a mesquite dune site. Agric. Forest Meteorol. 103, 249–264.
Massman, W.J., 1993. Errors associated with the combination method for estimating soil heat flux. Soil Sci. Soc. Am. J. 57, 1198–1202.
Mayocchi, C.L., Bristow, K.L., 1995. Soil surface heat flux: some general questions and comments on measurements. Agric. Forest Meteorl. 75, 43–50.
McCumber, M.C., Pielke, R.A., 1981. Simulation of the effects of surface fluxes of heat and moisture in mesoscale numerical model. 1. Soil layer. J. Geophys. Res. 86, 9929–9938.
Milly, P.C.D., 1982. Moisture and heat transport in hysteretic, inhomogeneous porous media: a matric head-based formulation and numerical model. Water Resour. Res. 18, 498.
Mitchell, R.L., Russell, J.W., 1971. Root development and root patterns of soybean (Glycine max (L.) Merrill) evaluated under field conditions. Agron. J. 63, 313–316.
Ochsner, T.E., Sauer, T.J., Horton, R., 2006. Field tests of the soil heat flux plate method and some alternatives. Agron. J. 98, 1005–1014.
Ochsner, T.E., Sauer, T.J., Horton, R., 2007. Soil heat capacity and heat storage measurements in energy balance studies. Agron. J. 99, 311–319.
Passerat de Silans, A., Bruckler, L., Thony, J.L., Vauclin, M., 1989. Numerical modeling of coupled heat and water flows during drying in stratified bare soil. Comparison with field observation. J. Hydrol. 105, 109–138.
Passerat de Silans, A., Monteny, B., Lhomme, J.P., 1997. The correction of soil heat flux measurements to derive an accurate surface energy balance by the Bowen ratio method. J. Hydrol. 188–189, 453–465.
Ren, T., Ochsner, T.E., Horton, R., 2003. Development of thermo-time domain reflectometry for vadose zone measurements. Vadose Zone J. 2, 544–551.
Sauer, T.J., Horton, R., 2005. Soil heat flux. In: Hatfield, J.L., Baker, J.M. (Eds.), Micrometeorology in Agricultural Systems. Agron. Monogr., 47. Am. Soc. of Agron, Madison, WI, pp. 131–154.
Shao, C., Chen, J., Li, L., Xu, W., Chen, S., Gwen, T., Xu, J., Zhang, W., 2008. Spatial variability in soil heat flux at three Inner Mongolia steppe ecosystems. Agric. Forest Meteorol. 148, 1433–1443.
Wang, J., Bras, R.L., 2009. Comment on "Estimating the soil temperature profile from a single depth observation: a simple empirical heatflow solution" by T.R.H Holmes et al. Water Resour. Res. 45, W03601.